Int. J. Electrochem. Sci., 16 **(2021)** Article ID: 210234, doi: 10.20964/2021.02.12

International Journal of
ELECTROCHEMICAL
SCIENCE
www.electrochemsci.org

Short Communication

Electrochemical non-enzymatic biosensor for tyramine detection in food based on silver-substituted ZnO nano-flower modified glassy carbon electrode

Fang Dong[1], *Ling Zhang*[1], *Ran Li*[1], *Zhongyuan Qu*[2], *Xiang Zou*[2,3], *Shaoqian Jia*[1,*]

[1] School of Health Sciences, Jiangsu Food & Pharmaceutical Science College, Huai'an, 223003, China
[2] School of Pharmacy, Harbin University of Commerce, Harbin, 150076, China
[3] School of Life Sciences, University of Sussex, Brighton, BN19RH, United Kingdom
[*]E-mail: jsspypdongfang@163.com

Received: 1 October 2020 / *Accepted:* 17 November 2020 / *Published:* 31 December 2020

This study focused on the preparation of Ag-substituted ZnO nano-flower modified GCE for determination of tyramine. Ag-substituted ZnO nano-flowers were synthesized through the spray pyrolysis method on GCE and their electrochemical properties of prepared electrodes were studied. Morphological analyses showed that the high porosity, high surface area and high density of nano-flower structures were synthesized on GCE. Structural analysis verified the substitution of Ag into the ZnO lattice of nano-flower which were grown in hexagonal wurtzite for ZnO and fcc phase of silver. EIS measurements showed that the *charge-transfer* resistance was decreased after the Ag substitution process which can be related to high conductivity of substituted silver on ZnO structure. CV analyses exhibited the stable response of modified GCE for determination of tyramine. The amperometry measurements displayed the fast response of Ag-substituted ZnO modified GCE to successive addition of tyramine solution which indicating the linear range, limit of detection and sensitivity were obtained 1-900 µM, 0.03 µM and 0.90281 µA/µM, respectively. Study on the interference effect showed selective and reliable response of Ag-substituted ZnO modified GCE for tyramine determination. Applicability of the prepared electrode was studied to determine tyramine in beer as a real sample which indicated the tyramine concentration in the real sample was 0.272 µM.

Keywords: Electrochemical impedance spectroscopy; Amperometry; Nano-flower**;** Silver-substituted ZnO; Tyramine detection

1. INTRODUCTION

Tyramine ($C_8H_{11}NO$) is most catecholamine releasing agent in foods that it usually found in plants and animals, and is metabolized by various monoamine oxidases. In foods, it is often derived from the decarboxylation of amino acid tyrosine in fermentation and decay process [1, 2]. It is not

observed in fresh foods but it level is increased by during storage and aging in room temperature [3, 4]. Therefore, the fermented, cured, pickled, aged, and spoiled foods contain high concentrations of tyramine [5]. For example, strong or aged cheeses (cheddar, Parmesan; Stilton, Gorgonzola, Camembert, feta, Muenster), cured, smoked, or processed meats (pepperoni, dry sausages, hot dogs, bologna, bacon, corned beef), and drinks (beer, vermouth, sherry, liqueurs) have high contents of tyramine [6-9].

Studies showed that high level tyramine in food can lead to headache, migraine, high blood pressure**,** hypertension, neurological and respiratory disorders [10, 11]. Therefore, the Agriculture Organization of the United Nations (FAO) and European Food Safety Authority (EFSA) considered tyramine as a hazard for foods [12-14]. Thus, many researches were conducted for development of fast, precise, sensitive, selective tyramine determination techniques in food samples. Very enzymatic and non-enzymatic tyramine sensors have been studied through thin layer chromatography [15], high pressure liquid chromatography [16], spectrophotometry [17], and electrochemical techniques such as amperometry, differential pulse voltammetry (DPV), cycle voltammetry (CV), linear sweep voltammetry (LSV) [18-23]. Among them the electrochemical techniques is an interesting and applicable method due to its cost, rapid and uncomplicated [24]. Many studies were carried out on MWCNT-AuNPs/chitosan/ molecularly imprinted polymer/GCE [25], indium tin oxide/3-aminopropyltriethoxysilane/reduced graphene oxide [26], carbon-fiber microelectrodes [20], carboxyl functionalized carbon nanotube [21] phosphate-doped polypyrrole film [27] and etc., for development of sensing properties of tyramine sensors and biosensors. These studies illustrated that modification of the electrode surface by nanostructure promotes sensitivity, stability and selectivity of sensor because of nanostructure's high aspect ratio and high porosity [28-30].

Accordingly, this study was conducted for the preparation Ag-substituted ZnO nano-flower modified GCE as non-enzymatic sensor and its application for electrochemical determination of tyramine through CV and amperometry techniques.

2. MATERIALS and METHOD

Ag-substituted ZnO nano-flower film was prepared through the spray pyrolysis method on glassy carbon electrodes. Before the preparation of film, the glassy carbon electrode (glassy carbon disk diameter of 2mm, Wuhan Corrtest Instruments Corp., Ltd., China) was mechanically polished successively with alumina slurry (99.5%, particle size of 1-5 μm, Hangzhou Jiupeng New Material Co., Ltd., China) on a polishing cloth for 20 minutes which followed by ultrasonication in deionized water for 10 minutes. 0.5 M zinc acetate (98%, Lianyungang Zhonghong Chemical Co., Ltd., China) solution was prepared in deionized water the silver acetate (99.99%, Sigma-Aldrich, UK) solution as a silver substitution source was added to zinc acetate solution. The silver concentration was 15 wt. %. The prepared solution was sprayed on the cleaned glassy carbon electrode at 350 °C. The spray pyrolysis deposition condition was kept constant and argon was applied as the carrier gas in the deposition process.

The morphology of prepared ZnO and Ag-substituted ZnO nano-flower modified GCE was analyzed by scanning electron microscopy (SEM, *JEOL-JSM-6010LA, Tokyo, Japan*). The crystalline structures of prepared samples were characterized by X-ray diffraction (XRD, *Bruker D2 Phaser*, Beerlika, MA, USA) operating at voltage of 35 kV and current of 10 mA with monochromatic wavelength radiation of CuKα (λ=1.5418 Å). Electrochemical impedance spectroscopy (EIS), cycle voltammetry (CV) and amperometry measurements were recorded by Autolab Potentiostat (PGStat 101, Metrohm Autolab, Utrecht, The Netherlands) with a conventional standard three-electrode electrochemical cell that Ag/AgCl electrode, Pt wire and prepared samples (prepared ZnO and Ag-substituted ZnO nano-flower modified GCE) were applied as the reference electrode, counter electrode and the working electrode, respectively. The electrolytes of electrochemical measurements were 0.1M *phosphate buffer solution (PBS) and* 0.1 M KCl (99.5%, Jinan Richnow Chemical Co., Ltd., China) solution which containing 5 mM $[Fe(CN)6]^{4-/3-}$ ($K_3Fe(CN)_6$, 99.5%, Shanghai Yancui Import And Export Corporation, China) solution. *PBS was prepared from* Na_2HPO_4 (99.0%, Shanghai Ruizheng Chemical Technology Co., Ltd., China). For preparation of the real sample, commercially available beer was provided from a local market and was added to 0.1 M PBS in volume ratio of 1:1.

3. RESULTS AND DISCUSSION

Figure 1 shows the SEM images of pure ZnO and Ag-substituted ZnO nano-flower films. As observed, there are nano-flower structures for both of the prepared films. The average diameter of nanorods are 180 nm and 230 nm, and average length of nanorods are 2.2 µm and 2.6 µm for pure ZnO and Ag-substituted ZnO nano-flower, respectively. The smooth surface of nanorods were found for pure ZnO and Ag substituted ZnO nano-flower films. Furthermore, the high porosity, high surface area and high density of petals are prepared on Ag-substituted ZnO nano-flower film surfaces.

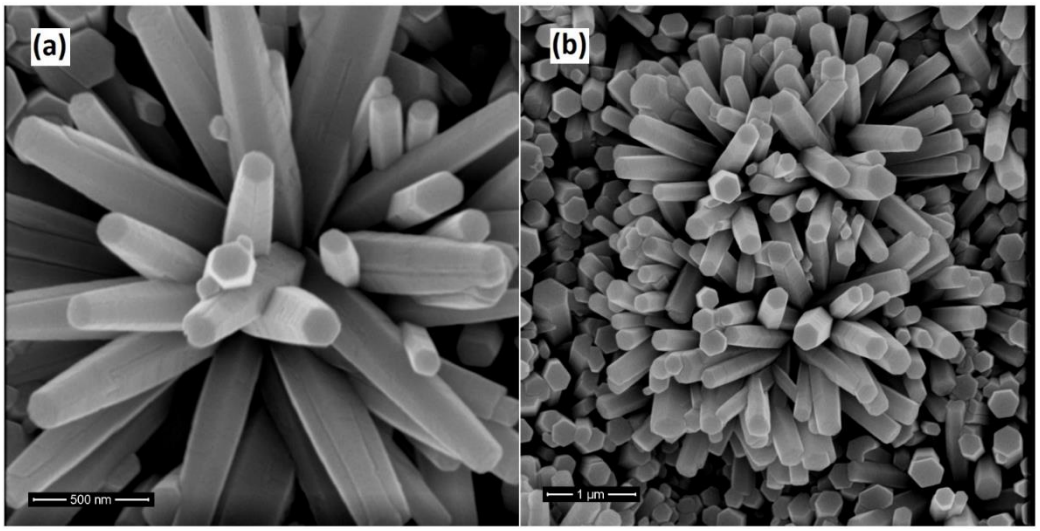

Figure 1. The SEM images of (a) pure ZnO and (b) Ag-substituted ZnO nano-flower films.

Figure 2 displays the recorded XRD patterns of pure ZnO and Ag-substituted ZnO films. As shown, all prepared films were grown in the crystalline phase of ZnO. There are diffraction peaks at 2θ = 32.12°, 34.58°, 36.66°, 47.77°, 57.08°, 63.14°, 68.19°, 10.18° and 77.29° are attributing to the growth along the (100), (002), (101), (102), (110), (103), (112), (004) and (202) directions, respectively which good agreement with formation of the hexagonal wurtzite for ZnO film (JCPDS card No. 075-1526) [31, 32]. For Ag-substituted ZnO film, the intensity of diffraction peak at (101) direction is decreased and intensity diffraction peak at (002) direction is increased. Moreover, two weak diffraction peaks at 2θ = 38.37°, 44.64°, 64.76° are associating with the (111), (200) and (220) planes, respectively which illustrating growth of the fcc phase of silver (JCPDS card No. 004-0783) that it is implying to the substitution of silver in ZnO lattice.

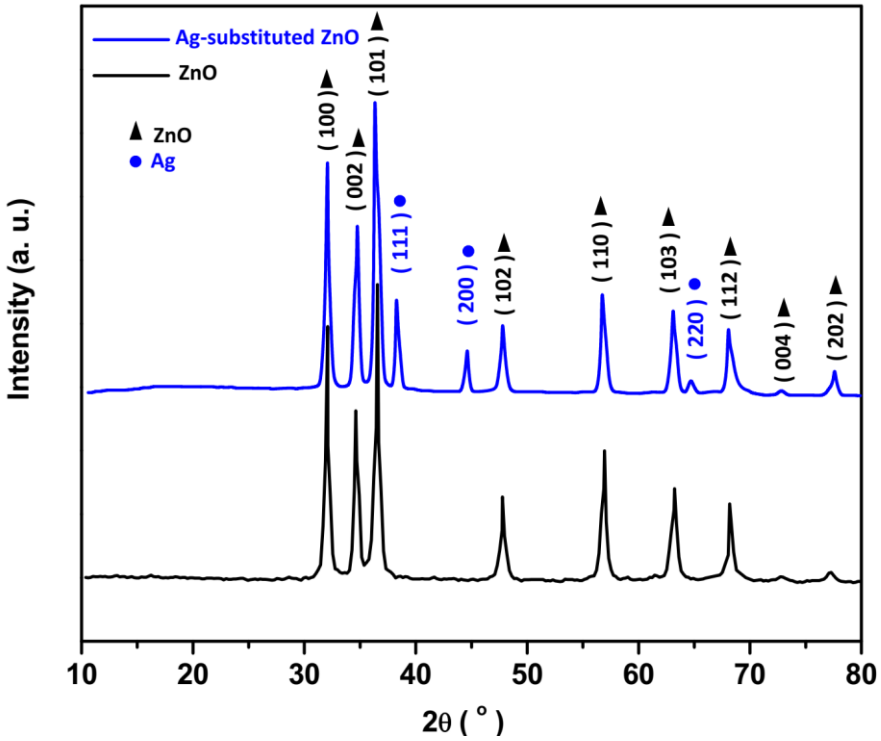

Figure 2. The recorded XRD patterns of pure ZnO and Ag-substituted ZnO films.

In order study the electron-transfer resistance at the electrode-solution interface for pure ZnO and Ag-substituted ZnO modifies GCE, the EIS measurements was recorded in 0.1 M KCl solution which containing 5 mM $[Fe(CN)6]^{4-/3-}$ solution as redox probe in the frequency range of 10^{-1} Hz to 10^{5} Hz at AC voltage amplitude of 5 mV. As seen in Figure 3, the Nyquist plots exhibit the semicircle curve part at high frequencies that is related to the charge-transfer resistance (R_{ct}) which can be indicated by radius of semicircle [33-35]. Moreover, the Nyquist plots also show an inclined line part at low frequencies which is controlled by diffusion. Thus, the charge-transfer resistance of pure ZnO and Ag-substituted ZnO modifies GCE can be obtained of 0.503 kΩ and 0.368 kΩ, respectively. It is indicated the charge-transfer resistance is decreased after the substitution process which can be related

to high conductivity of substituted silver on ZnO structure [36]. Therefore, lower charge-transfer resistance of Ag-substituted ZnO film can provide a high electron transfer rate between the electrolyte and electrode surface.

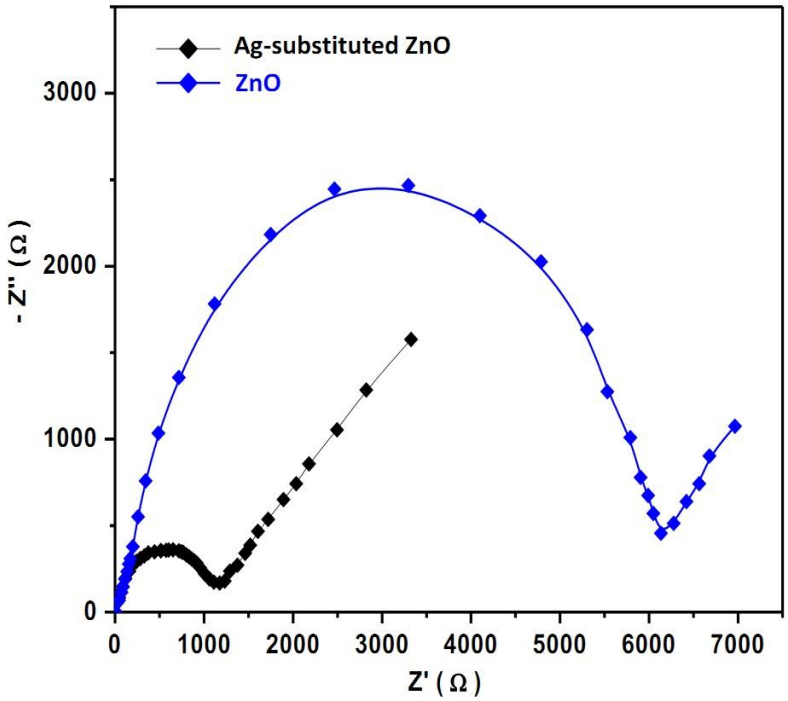

Figure 3. The recorded Nyquist plots of pure ZnO and Ag-substituted ZnO films in 0.1 M KCl solution which containing 5 mM $[Fe(CN)6]^{4-/3-}$ solution in the frequency range of 10^{-1} Hz to 10^{5} Hz at AC voltage amplitude of 5 mV.

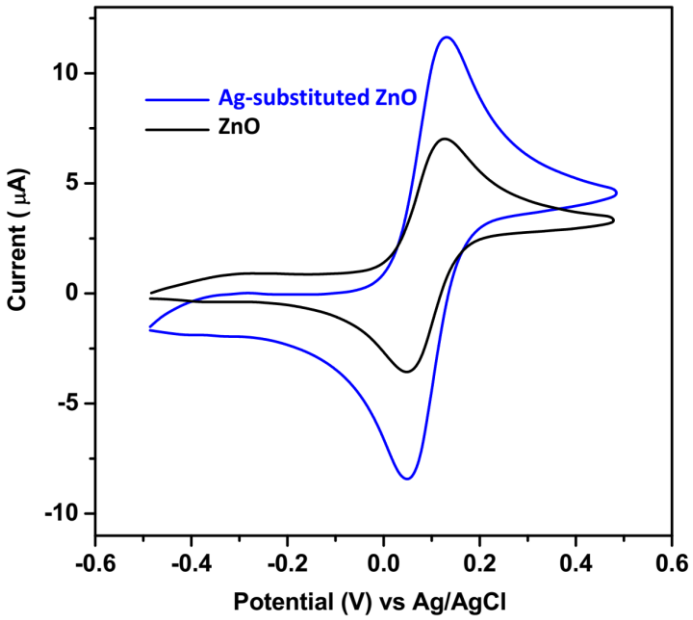

Figure 4. The recorded CVs of pure ZnO and Ag-substituted ZnO films in 0.1 M KCl solution which containing 5 mM $[Fe(CN)6]^{4-/3-}$ solution at scan rate of 10 mVs^{-1} and potential range of -0.5 V to 0.5 V.

Further electrochemical study of prepared pure and substituted ZnO modified GCE was conducted through CV technique. The CVs of the electrodes were recorded in mixture of 0.1 M KCl and 5 mM $[Fe(CN)6]^{4-/3-}$ solutions at scan rate of 10 mVs^{-1} and potential range of -0.5 V to 0.5 V. As observed Figure 4, both of electrodes show the well-defined redox peaks. It is observed that difference potential between anodic and cathodic peaks (ΔE) are obtained 0.077 and 0.069 V for pure and substituted ZnO modified GCE, respectively. Furthermore, the Ag-substituted ZnO modified GCE shows the higher current for the anodic and cathodic peaks than pure ZnO modified GCE because of its lower electron transfer resistance at the electrode-solution interface. The substitution process improves the conductivity and surface area of the film. Therefore, the following electrochemical studies were carried out on Ag-substituted ZnO modified GCE surfaces.

The CV response of Ag-substituted ZnO modified GCE was recorded in 0.1 M PBS pH 7.0 at scan rate of 10 mVs^{-1} and potential range of -0.5 V to 1.0 V in presence and absence of 10 µM tyramine. Figure 5 shows that the both of recorded CVs exhibit the peak at 0.20 V for silver [37]. Moreover, there is a single oxidation peak at 0.7 in presence of 10 µM tyramine. In addition, the stability of electrochemical response was investigated through the record of successive CVs. Figure 6 shows first and 100^{th} recorded CVs in presence of 10 µM tyramine that exhibits 6 % changes for current of tyramine oxidation peak which indicate the stability response of Ag-substituted ZnO modified GCE for determination of tyramine.

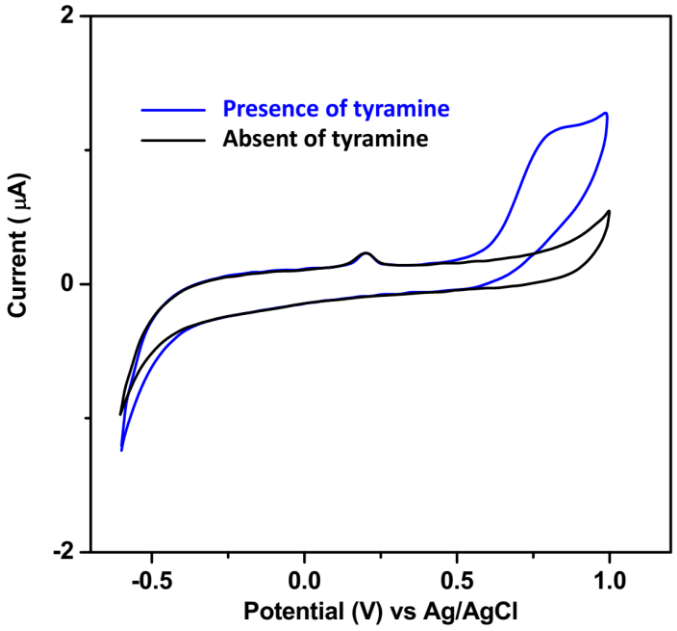

Figure 5. The recorded CV response of Ag-substituted ZnO modified GCE in 0.1 M PBS pH 7.0 at scan rate of 10 mVs^{-1} and potential range of -0.5 V to 1.0 V in presence and absent of 10 µM tyramine.

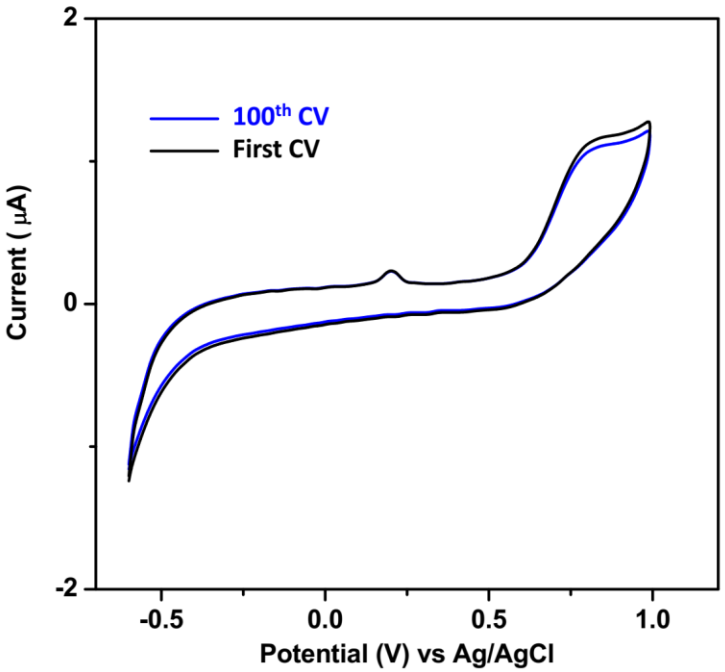

Figure 6. The first and 100th recorded CVs response of Ag-substituted ZnO modified GCE in 0.1 M PBS pH 7.0 at scan rate of 10 mVs^{-1} and potential range of -0.5 V to 1.0 V in presence of 10 µM tyramine.

The amperometry technique was applied to estimate the linear range, sensitivity and limit of detection of Ag-substituted ZnO modified GCE for determination of tyramine. Figure 7 depicts the recorded amperogaram response and the calibration plot of Ag-substituted ZnO modified GCE in 0.1 M PBS pH 7.0 at 0.7 V and rotating speed of 1000 rpm. As seen, the fast response of Ag-substituted ZnO modified GCE was recorded after successive addition of 1 µM tyramine solution and current responses were increased linearly with addition of tyramine solution. The limit of detection and sensitivity on Ag-substituted ZnO modified GCE surfaces were obtained 0.03 µM and 0.90281 µA/µM, respectively. For determination of linear range of sensor, the amperometry study was also performed for successive addition of 100 µM tyramine solution and its calibration plot is shown in Figure 8 which indicating linear range for determination of tyramine on Ag-substituted ZnO modified GCE was 1-900 µM.

Table 1 presents the linear range, limit of detection and sensitivity of reported in literature for tyramine determination. Comparison with the summarized properties of tyramine sensors in Table 1 shows that the Ag-substituted ZnO modified GCE exhibits high sensitivity and wide linear range response for tyramine determination.

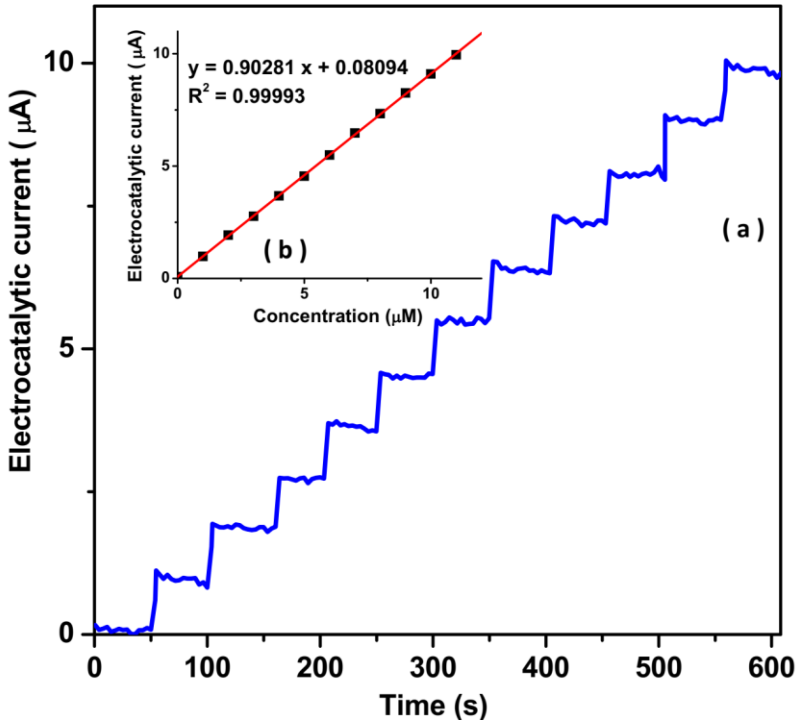

Figure 7. (a) The recorded amperogaram response of Ag-substituted ZnO modified GCE in 0.1 M PBS pH 7.0 at 0.7 V and rotating speed of 1000 rpm in successive addition of 1 µM tyramine solution and (b) calibration plot.

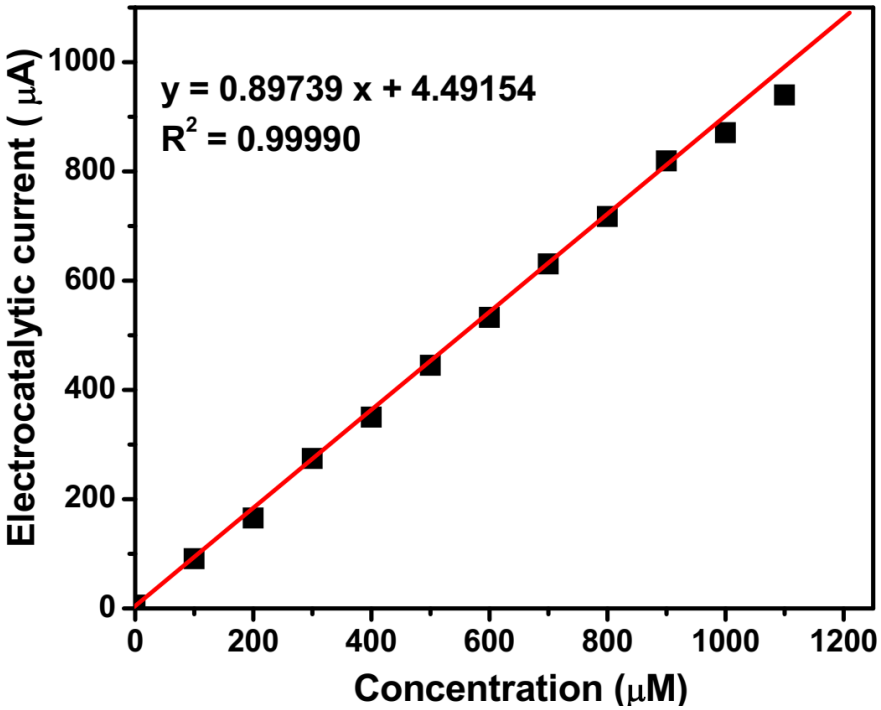

Figure 8. The calibration plot of Ag-substituted ZnO modified GCE in 0.1 M PBS pH 7.0 at 0.7 V and rotating speed of 1000 rpm in successive addition of 100 µM tyramine solution.

Table 1. Comparison of the sensing properties of Ag-substituted ZnO modified GCE with other reported literature for determination tyramine.

Electrode	Technique	Linear Range (µM)	limit of detection (µM)	Sensitivity (µA/µM)	ref
Ag-substituted ZnO modified GCE	Amperometry	1-900	0.03	0.90281 0.89739	This work
MWCNT-AuNPs/chitosan/ molecularly imprinted polymer /GCE	Amperometry	0.3-10	0.057	-	[25]
Indium tin oxide/3-aminopropyltriethoxysilane/ reduced graphene oxide	DPV	1-100	0.0001	0.2137	[26]
Carbon-fiber microelectrodes	CV	0.1–10	0.057	-	[20]
Carboxyl functionalized carbon nanotube	Amperometry	5–180	0.62	0.7414	[21]
Phosphate-doped polypyrrole film	Amperometry	4–80	0.57	0.1069	[27]

Interference response of Ag-substituted ZnO modified GCE was studied for tyramine determination through amperometry technique in the addition of various substances. Table 2 presents the recorded electrocatalytic currents response of Ag-substituted ZnO modified GCE in 0.1 M PBS pH 7.0 at 0.7 V in successive additions of 1 µM tyramine solution and 10 µM of various substances. As observed, the modified electrode illustrates significant electrocatalytic currents to additions of tyramine solution and there are not any considerable recorded electrocatalytic currents for the additions of other substances.

Table 2. The recorded electrocatalytic currents response of Ag-substituted ZnO modified GCE in 0.1 M PBS pH 7.0 at 0.7 V in successive additions of 1 µM tyramine solution and 10 mM of various substances.

Specie	Added (µM)	Electrocatalytic current density (µA)	RSD (%)
tyramine	1	0.913	±0.013
Mg^{2+}	10	0.011	±0.008
Ca^{2+}	10	0.014	±0.009
llysine	10	0.013	±0.007
l-cysteine	10	0.021	±0.009
l-asparagines	10	0.017	±0.007
N-acetyl-l-cysteine	10	0.011	±0.008
glycine	10	0.015	±0.005
phenylalanine	10	0.016	±0.008
glutathione	10	0.019	±0.009

Therefore, the summarized substances in Table 2 do not interfere with detection of Gallic acid on Ag-substituted ZnO modified GCE surface. Moreover, the recorded response of modified to addition tyramine shows that there is selectivity and reliable response to addition tyramine on modified electrode surfaces.

Applicability of the Ag-substituted ZnO modified GCE was studied to tyramine determination in prepared real sample of beer through amperometry technique in pH 7.0 at 0.7 V. Figure 9 presents the recorded amperogaram response of modified GCE in successive addition of 1 µM tyramine solution and calibration plot. Therefore, the tyramine concentration in solution of cell and beer are obtained 0.136 µM and 0.272 µM, respectively. Furthermore, Analytical applicability of the Ag-substituted ZnO modified GCE was also evaluated to determine tyramine in beer samples. The results of this study are presented in Table 3 which indicates the obtained recovery (more than 83.00%) and relative standard deviation **(**RSD) (less than 2.81%) values are acceptable. Accordingly, the results show the reliable application of Ag-substituted ZnO modified GCE for the determination of tyramine in food samples.

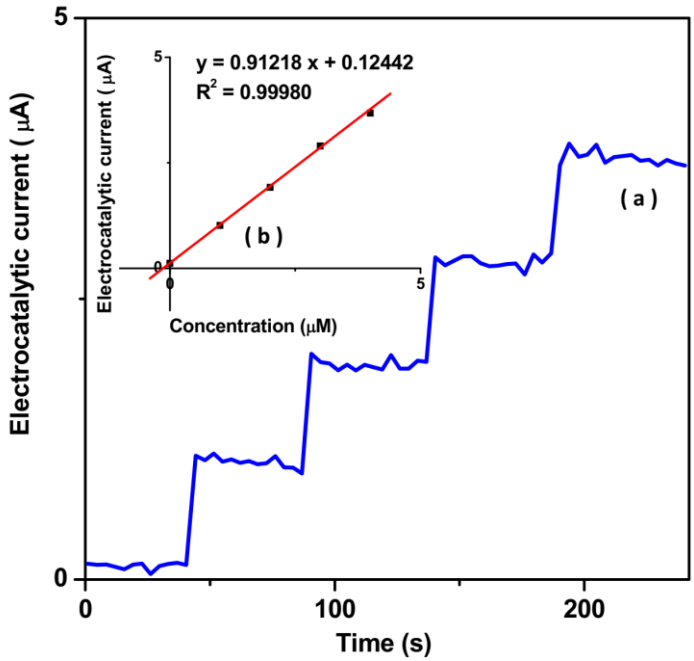

Figure 9. (a) The recorded amperogaram response of Ag-substituted ZnO modified GCE in prepared real sample of beer pH 7.0 at 0.7 V and rotating speed of 1000 rpm in successive addition of 1 µM tyramine solution and (b) calibration plot .

Table 3. Results of practical determination of tyramine in beer samples (n = 5)

Sample	Added (µM)	Fund (µM)	Recovery (%)	RSD (%)
beer	1.00	0.83	83.00	2.11
	2.00	1.78	89.00	2.82
	3.00	2.85	95.00	2.10
	4.00	3.65	91.25	1.25
	5.00	4.68	93.60	1.97

4. CONCLUSION

In this work, Ag-substituted ZnO nano-flower modified GCE was studied for determination of tyramine. Ag-substituted ZnO nano-flowers were prepared through the spray pyrolysis method on GCE. The SEM, XRD, EIS, CV and amperometry analyses were applied to characterize the structural and electrochemical properties of prepared electrodes. Results showed that the high porosity, high surface area and high density of nano-flower structures were synthesized on GCE. XRD analysis of nano-flower indicated the substitution of silver in ZnO lattice and nano-flowers were grown in hexagonal wurtzite for ZnO and fcc phase of silver. EIS measurements showed that the charge-transfer resistance was decreased after the silver substitution process which can be related to high conductivity of substituted silver on ZnO structure. CV measurements exhibited the stable response of Ag-substituted ZnO modified GCE for determination of tyramine. The amperometry measurements displayed the fast response of Ag-substituted ZnO modified GCE to successive addition of tyramine solution which indicate the linear range, limit of detection and sensitivity were obtained 1-900 µM, 0.03 µM and 0.90281 µA/µM, respectively. Comparison sensing properties of prepared electrode with the other reported literature revealed that the Ag-substituted ZnO modified GCE exhibited high sensitivity and wide linear range response for tyramine determination. Study on the interference effect illustrated that prepared electrodes show selective and reliable response for tyramine determination. Applicability of the Ag-substituted ZnO modified GCE was studied to determine tyramine in beer as real sample through amperometry which indicates the tyramine concentration in real sample was 0.272 µM.

ACKNOWLEDGMENTS
This work was supported by Cyan Engineering Grant Program of Jiangsu Province for Key Teacher in University, China(No. 2018[12]) and Natural Science Foundation of Huai'an, Jiangsu Provence, China (no. HAB201840).

Refereces

1. L. Wang, X. Hui, H. Geng, L. Ye, A.-y. Zhang, Z. Shao and Z.-g. Feng, *Colloid and Polymer Science*, 295 (2017) 1549.

2. R. Mohamed, J. Rouhi, M.F. Malek and A.S. Ismail, *International Journal of Electrochemical Science*, 11 (2016) 2197.
3. J. Rouhi, S. Mahmud, N. Naderi, C.R. Ooi and M.R. Mahmood, *Nanoscale research letters*, 8 (2013) 1.
4. H. Karimi-Maleh, F. Karimi, S. Malekmohammadi, N. Zakariae, R. Esmaeili, S. Rostamnia, M.L. Yola, N. Atar, S. Movagharnezhad and S. Rajendran, *Journal of Molecular Liquids*, 310 (2020) 113185.
5. Z. Shamsadin-Azad, M.A. Taher, S. Cheraghi and H. Karimi-Maleh, *Journal of Food Measurement and Characterization*, 13 (2019) 1781.
6. B. Dalkıran, P.E. Erden, C. Kaçar and E. Kılıç, *Electroanalysis*, 31 (2019) 1324.
7. D. Zhang, H. Liu, W. Geng and Y. Wang, *Food chemistry*, 277 (2019) 639.
8. T.J. Bruce and S.A. Saeed, *American Family Physician*, 60 (1999) 2311.
9. M. Alimanesh, J. Rouhi and Z. Hassan, *Ceramics International*, 42 (2016) 5136.
10. B. del Rio, B. Redruello, D.M. Linares, V. Ladero, M. Fernandez, M.C. Martin, P. Ruas-Madiedo and M.A. Alvarez, *Food chemistry*, 218 (2017) 249.
11. J. Rouhi, S. Mahmud, S. Hutagalung and S. Kakooei, *Micro & Nano Letters*, 7 (2012) 325.
12. D.M. Linares, B. del Rio, B. Redruello, V. Ladero, M.C. Martin, M. Fernandez, P. Ruas-Madiedo and M.A. Alvarez, *Food chemistry*, 197 (2016) 658.
13. L. Nan, C. Yalan, L. Jixiang, O. Dujuan, D. Wenhui, J. Rouhi and M. Mustapha, *RSC Advances*, 10 (2020) 27923.
14. M. Miraki, H. Karimi-Maleh, M.A. Taher, S. Cheraghi, F. Karimi, S. Agarwal and V.K. Gupta, *Journal of Molecular Liquids*, 278 (2019) 672.
15. J.C.R. Gonzalo, C.G. Moreno, A.G. Cerro and A.M. Font, *Journal of the Association of Official Analytical Chemists*, 62 (1979) 272.
16. P. Koehler and R. Eitenmiller, *Journal of Food Science*, 43 (1978) 1245.
17. C.S. Evans, S. Gray and N.O. Kazim, *analyst*, 113 (1988) 1605.
18. M. Baghayeri, H. Beitollahi, A. Akbari and S. Farhadi, *Russian Journal of Electrochemistry*, 54 (2018) 292.
19. V.S. Sapner, P.P. Chavan, R.V. Digraskar, S.S. Narwade, B.B. Mulik, S.M. Mali and B.R. Sathe, *ChemElectroChem*, 5 (2018) 3191.
20. S.E. Cooper and B.J. Venton, *Analytical and Bioanalytical Chemistry*, 394 (2009) 329.
21. I.M. Apetrei and C. Apetrei, *Journal of Food Engineering*, 149 (2015) 1.
22. J. Rouhi, C.R. Ooi, S. Mahmud and M.R. Mahmood, *Electronic Materials Letters*, 11 (2015) 957.
23. H. Karimi-Maleh, M. Sheikhshoaie, I. Sheikhshoaie, M. Ranjbar, J. Alizadeh, N.W. Maxakato and A. Abbaspourrad, *New Journal of Chemistry*, 43 (2019) 2362.
24. Z. Savari, S. Soltanian, A. Noorbakhsh, A. Salimi, M. Najafi and P. Servati, *Sensors and Actuators B: Chemical*, 176 (2013) 335.
25. J. Huang, X. Xing, X. Zhang, X. He, Q. Lin, W. Lian and H. Zhu, *Food Research International*, 44 (2011) 276.
26. M.Z.H. Khan, X. Liu, J. Zhu, F. Ma, W. Hu and X. Liu, *Biosensors and Bioelectronics*, 108 (2018) 76.
27. I.M. Apetrei and C. Apetrei, *Sensors and Actuators B: Chemical*, 178 (2013) 40.
28. R. Savari, H. Savaloni, S. Abbasi and F. Placido, *Sensors and Actuators B: Chemical*, 266 (2018) 620.
29. F. Chahshouri, H. Savaloni, E. Khani and R. Savari, *Journal of Micromechanics and Microengineering*, 30 (2020) 075001.
30. S. Changaei, J. Zamir-Anvari, N.-S. Heydari, S.G. Zamharir, M. Arshadi, B. Bahrami, J. Rouhi and R. Karimzadeh, *Journal of Electronic Materials*, 48 (2019) 6216.
31. H. Savaloni and R. Savari, *Materials Chemistry and Physics*, 214 (2018) 402.

32. J. Rouhi, S. Kakooei, S.M. Sadeghzadeh, O. Rouhi and R. Karimzadeh, *Journal of Solid State Electrochemistry*, 24 (2020) 1599.
33. L. Wang, J. Zhao, X. He, J. Gao, J. Li, C. Wan and C. Jiang, *International Journal of Electrochemical Science* 7(2012) 345.
34. Y.-L. Shi, M.-F. Shen, S.-D. Xu, X.-Y. Qiu, L. Jiang, Y.-H. Qiang, Q.-C. Zhuang and S.-G. Sun, *International Journal of Electrochemical Science* 6(2011) 3399.
35. R. Dalvand, S. Mahmud and J. Rouhi, *Materials Letters*, 160 (2015) 444.
36. M. Karyaoui, D. Ben Jemia, M. Gannouni, I. Ben Assaker, A. Bardaoui, M. Amlouk and R. Chtourou, *Inorganic Chemistry Communications*, 119 (2020) 108114.
37. N. Couzon, M. Maillard, L. Bois, F. Chassagneux and A. Brioude, *The Journal of Physical Chemistry C*, 121 (2017) 22147.